Available online at www.sciencedirect.com
SCIENCE DIRECT
Biochimica et Biophysica Acta 1760 (2006) 922–929
BIOCHIMICA ET BIOPHYSICA ACTA
BBA
http://www.elsevier.com/locate/bba

Differences in the biophysical properties of membrane and cytoplasm of apoptotic cells revealed using dielectrophoresis

Fatima H. Labeed [a,b], Helen M. Coley [b], Michael P. Hughes [a,*]

[a] Centre for Biomedical Engineering, School of Engineering, University of Surrey, Guildford, Surrey GU2 7XH, UK
[b] Division of Oncology, Postgraduate Medical School, University of Surrey, Guildford, Surrey GU2 7XH, UK

Received 30 July 2005; received in revised form 30 January 2006; accepted 30 January 2006
Available online 23 February 2006

Abstract

We have used dielectrophoresis to determine the dielectric properties of human chronic myelogeneous leukaemic (K562) cells during apoptosis (programmed cell death). Our results indicate that K562 cells increase markedly in cytoplasmic conductivity from 0.28 S/m to 0.50 S/m within the first 4 h following treatment with staurosporine, which then lasts beyond 12 h, whilst cell shrinkage increases the capacitance of the membrane from 9.7 mF/m^2 to 20 mF/m^2. After 24 and 48 h of incubation with staurosporine, multiple sub-populations were detected, highlighted by the dielectric changes that the cell undergoes before death. By comparing these results with those obtained by common apoptosis monitoring techniques Annexin V and TMRE (tetramethylrhodamine ethylester), it is possible to infer the role of ion efflux in the progress of apoptosis. The use of dielectrophoresis for monitoring apoptosis offers a number of benefits as it is both rapid and non-invasive. It can also be used in parallel with other assays in high-throughput screening applications.

Keywords: Dielectrophoresis; Apoptosis; Cytoplasm; Annexin; TMRE; k562

1. Introduction

Apoptosis is a process that plays a critical role in the embryonic stage of development and in tissue homeostasis. In humans, dysfunction of this process has been linked to pathogenesis of cancer and other diseases [1]. The term was first described in a landmark paper [2] in which Kerr and colleagues described the morphological features of cell death, characterised by nuclear and cytoplasmic shrinkage. The morphological changes in apoptotic and necrotic cells have been described [3], where in apoptotic cells the main changes occur in the nuclear compartment with initial marked condensation in the chromatin. This is accompanied by convolution in the nuclear and cellular outlines and nuclear fragmentation. Surface protuberances separate out from the plasma membrane and then re-seal to form membrane-*bound apoptotic bodies* that may or may not contain nuclear fragments. Due to cell shrinkage, the cell also loses its normal cell contacts and some surface elements, such as microvilli and cell–cell junctions, well before cellular budding and fragmentation take place.

The mitochondrion is central to the apoptotic process, as it controls the release of multiple death-triggering proteins that lead to the execution phase of apoptosis, as reviewed by Green and Reed [4]. In addition to the liberation of pro-apoptotic factors and activation of the caspase cascade, a typical early characteristic of apoptosis is mitochondrial membrane permeabilisation followed by dissipation of the mitochondrial transmembrane potential ($\Delta\psi_m$). Disruption of $\Delta\psi_m$ has been detected in cells undergoing apoptosis, indicating permeability transition pore (PT) opening, using assay techniques such as TMRE. However, the exact relationship (such as cause or consequence) between $\Delta\psi_m$ and release of apoptotic factors is still a matter of debate.

Ion flux across the plasma membrane has also been found to be a significant part of the apoptotic process. For example, Khaled and colleagues [5] found that early stress-related events preceded cell death. Intracellular rise in pH (alkalinisation) took

* Corresponding author. Tel.: +44 1483 686775; fax: +44 1483 689395.
E-mail address: m.hughes@surrey.ac.uk (M.P. Hughes).

0304-4165/$ - see front matter © 2006 Elsevier B.V. All rights reserved.
doi:10.1016/j.bbagen.2006.01.018

place peaking above pH 7.8 2–3 h post interleukin-3 withdrawal, and induced a transient increase in the $\Delta\psi_m$. The authors noticed a sharp decline of ATP during this early period, and suggested that the rise in the intracellular pH inhibited the mitochondrial import of ADP, which consequently limits ATP production. The inhibition of the ADP import into the mitochondria causes the activation of proton pumps in the membrane, which consume ATP and pump out protons, raising $\Delta\psi_m$. In cytokine withdrawal-induced apoptosis, intracellular alkalinisation was observed and was suggested to be mediated by pH regulator Na^+/H^+ exchanger (NHE1). Another study [6] suggested the rise in cytosolic pH to be mediated by the Cl^-/HCO_3^- anion exchanger, where Cl^- ions are moving out in exchange for HCO_3^- ions moving in. The ionic influx/efflux plays an important role in apoptosis and some ions mediate the change in cell volume. The principal ion is K^+, where its intracellular concentration has been widely reported to be diminished during the apoptotic process. K^+ is pumped out of the cell and cell shrinkage takes place, and the role of this ion is pivotal in the cell death programme [7–9]. Also, a transient increase in intracellular Na^+ has been reported prior to the loss of cell volume [10]. An increased generation of reactive oxygen species has been reported [11], which leads to the transient increase in $\Delta\psi_m$. At later stages of apoptosis, the $\Delta\psi_m$ was found to decrease as the mitochondria depolarises. In these late stages, massive Ca^{2+} influx takes place [12], as well as mitochondrial swelling prior to cell lysis [13].

AC-electrokinetic techniques such as dielectrophoresis (DEP) and electrorotation (ROT) use the motion of cells in non-uniform, time-variant electric fields [14–16] to study dielectric properties of both the membrane and cytoplasm for a number of biological particles in a cancer setting [17–26]. In this paper, we examine the use of DEP to shed light on these findings by looking at the changes in the dielectric properties over a period of 48 h following induction of apoptosis in K562 cells using staurosporine. A prior study [27] demonstrated the use of DEP in detecting changes in membrane dielectric properties of cultured human promyelocytic leukaemia cells (HL-60) during the early stages of apoptosis after treatment with the compound genistein. We extended this by examining changes in both the cytoplasm and membrane over longer incubation periods with staurosporine, and demonstrate that a broader range of effects can be observed in multiple subpopulations simultaneously using DEP.

2. Materials and methods

2.1. Cell culture and the induction of apoptosis

Staurosporine (Alexis Corporation, Nottingham, UK) was dissolved in dimethyl sulfoxide (DMSO), and stored frozen as a 1 mM stock solution and thawed prior to use. Human chronic myelogenous leukaemia (K562) cells were cultured under the same conditions described by Labeed and colleagues [26]. Briefly, cells were grown in 20 mM HEPES modified RPMI-1640 medium supplemented with 10% heat-inactivated foetal calf serum (FCS), (Invitrogen, Paisley, UK), 2 mM L-glutamine and 100 units/mL penicillin-streptomycin, in a standard cell culture incubator at 5% CO_2 and 37 °C. All cell culture reagents were obtained from Sigma Aldrich (Poole, UK), unless stated otherwise.

The cells were treated with an apoptosis inducing agent (staurosporine) at 1 mM or 2 mM depending on the density of cells and incubation period used. The incubation period included five time points (4, 8, 12, 24 and 48 h). For the earlier incubation time points (4 and 8 h), a density of 6×10^5/mL at 1 μM staurosporine was used. For the later time points (12, 24 and 48 h), a density of 3×10^5/mL at 2 mM was used. This procedure was adopted in order to account for cell growth encountered in cultures at the longer time points and to have enough pharmacological exposure to staurosporine.

2.2. DEP experiments

K562 cells were centrifuged at room temperature at 190×*g* for 5 min. The pellet was washed and resuspended twice (to ensure removal of culture medium) in isotonic medium consisting of 8.5% (w/v) sucrose plus 0.3% (w/v) dextrose buffer [22]. The final conductivity of the medium was adjusted to 5 mS/m using PBS and the final conductivity, before use, was verified with a conductivity meter (RS components Ltd, London, UK). The final cell population, depending on the incubation time point used, was counted using a haemocytometer and adjusted to approximately 3×10^5 cells/mL (±15%) for DEP measurements. Signals of 10 V_{pk-pk} and frequencies between 5 kHz and 20 MHz (at 5 frequencies per decade) were used. The experiments were repeated 4–6 times with different populations, which were summed prior to modelling. The experimental set up and electrode arrangement were used as described by Labeed and colleagues [26], as shown in Fig. 1. Cells were used immediately after resuspension to minimise the experimentation time; performing experiments in reverse order of frequency indicated that no changes occurred in the spectrum due to period of time in suspension during the course of the experiment. Cells were collected at the electrodes for a period of 1 min,; collection was observed by microscope and video camera/monitor, and cells were counted as they collected. Since cell repulsion cannot be quantified by this method, only positive (attractive) dielectrophoresis was observed.

2.3. Flow cytometry

2.3.1. Annexin V assay

In normal viable cells, the phosphatidylserine (PS) molecules are located on the cytoplasmic surface of the cell membrane. When apoptosis occurs, rapid alterations in the organisation of the phospholipids can occur leading to the exposure of PS on the cell surface [28,29]. For these experiments, the rapid Annexin V-FITC detection kit (CN Biosciences, Beeston, UK) was used in accordance with the manufacturer's instructions. The assay principle uses FITC-conjugate Annexin V to detect PS exposure by flow cytometry. Simultaneously, propidium iodide (PI) was used to distinguish viable, necrotic or apoptotic cells in the late terminal stages, as PI is only internalised in cells whose membranes have become permeable.

A population of around 0.5×10^6 cells in culture media was used for each experiment. The analysis was performed using a Coulter Epics XL flow

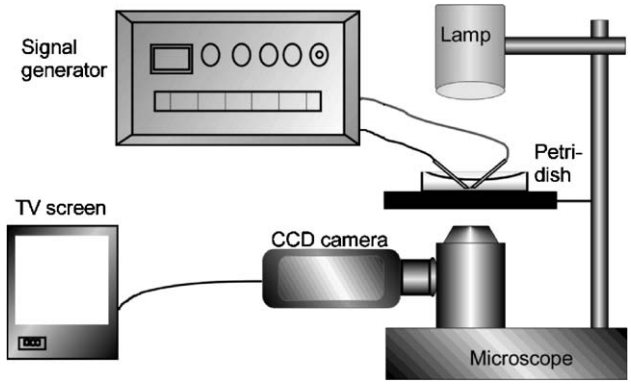

Fig. 1. A schematic representation of the experimental setup used for DEP measurements. A signal generator was used to supply an AC voltage to the electrodes. Observations were made using a video camera connected to a television and video recorder for data collection and analysis.

cytometer emitting an excitation laser light at 488 nm. Fluorescence was measured at 518 nm and at 620 nm for FITC and PI detection. Adjustments were made to minimise overlap between these two measurements.

2.3.2. TMRE (tetramethylrhodamine ethylester) assay

TMRE (Invitrogen, Paisley, UK) is a highly fluorescent permeant cationic, lipophilic dye. It is used as a fluorescent probe to monitor the membrane potential of mitochondria, as it accumulates in the negatively charged mitochondrial matrix according to the Nernst equation potential [30]. TMRE stock was prepared at a concentration of 1 mM made with DMSO and stored at −20°C to make a working solution of 10 μM. The cultured K562 cells, at a density of approximately 2.5×10^5/mL were grown overnight and then treated with 1 μM staurosporine on the following day. Cells were exposed to the drug for a number of hours as indicated by the time points used. After each time point, the cells were centrifuged at 200×*g* for 3 min and the pellet was resuspended in a medium containing PBS supplemented with 2 g/L D-glucose. This was done in order to reproduce standard cell culture conditions. The cells were then incubated with TMRE (at a final 100 nM concentration) for 40 min away from light, and again under the normal cell culture conditions. The cells were centrifuged at 200×g for 3 min, after which the pellet was resuspended in 500 μL of the PBS medium (with 2 g/L D-glucose). A positive control TMRE sample was also prepared, which involved following the same procedure described earlier, except that an uncoupler carbonyl cyanide m-chlorophenylhydrazone (CCCP) was added at 10 μM final concentration before adding 100 nM TMRE to the cells. The cells were then incubated for 3 min at room temperature in darkened conditions. All samples were then analysed by flow cytometry. CCCP is a protonophore, which depolarises the mitochondria by abolishing the proton gradient across the inner mitochondrial membrane [31,32], producing a leftward shift on the peak with respect to cells with TMRE but without staurosporine (data not shown). In order to assess the mitochondrial membrane potential, the shift in the fluorescence peak was compared with the control cells (with TMRE but not staurosporine) and to that of positive control cells. The peak shift gives an indication of the extent of mitochondrial membrane hyperpolarisation or depolarisation (causing a shift of the peak value up or down, respectively).

3. Results

The three assays were used on cell suspensions following 4, 8, 12, 24 and 48 h of exposure to staurosporine. The observations using all three indicated that similar patterns of results were seen for the early (4–12 h) and late (24–48 h) stages of apoptotic progression. Figs. 2–4 show examples of the data by all three methods for the control sample prior to staurosporine treatment, and 4 h and 24 h after initial exposure respectively. Table 1 summarises the biophysical properties of K562 before and after treatment with staurosporine, as determined with best-fit modelling of the collection data using a single-shell model as described by Labeed and colleagues [26]. The results shown in these figures, and the parameters calculated from the data, have been the average of at least 6 experiments. As reported by Broche and colleagues [33], the cytoplasmic permittivity cannot be reliably determined, but the frequency at which the collection declines gives a direct indication of the cytoplasmic conductivity of the cells in the sample.

After treatment with staurosporine, significant changes were seen in the cytoplasmic conductivity at different time points. After 4 h of treatment, the cells were showing signs of mitochondrial membrane hyperpolarisation, as the cytoplasmic conductivity increased from 0.28 to 0.40 S/m following staurosporine treatment. Hence, the data were

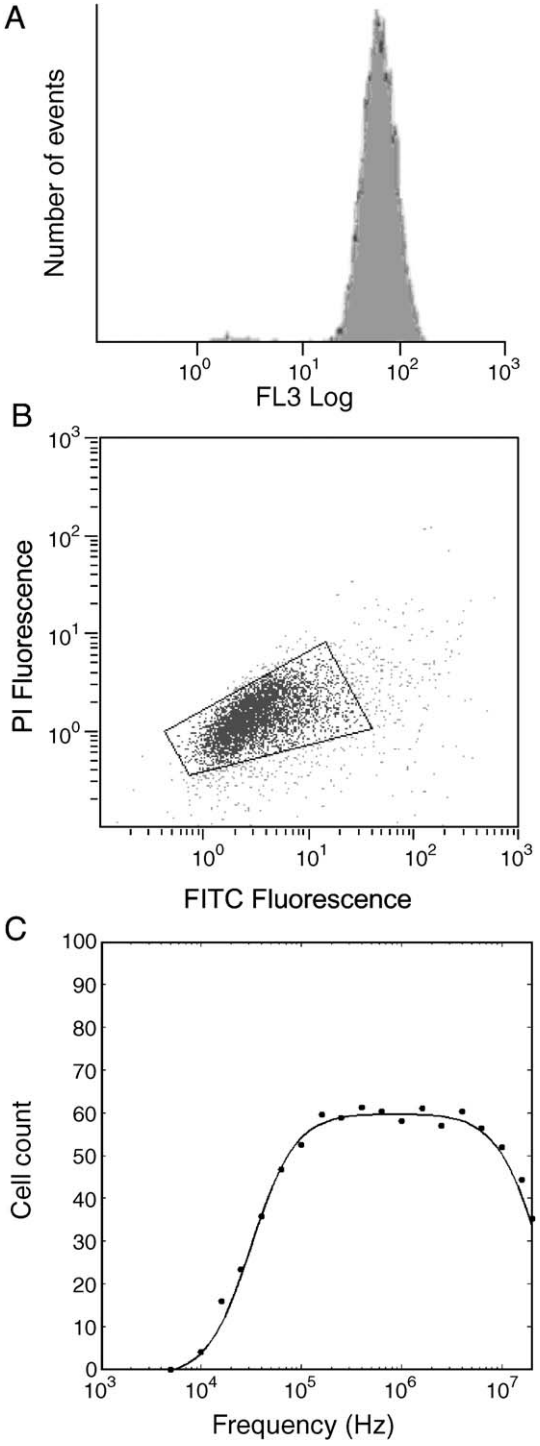

Fig. 2. The TMRE (A), Annexin-V (B) and DEP spectrum data (C) for the control sample of cells without staurosporine treatment.

suggestive of an increase in the ionic concentration of the cytoplasm after 4 h of incubation with staurosporine. The hyperpolarisation pattern appeared to continue at this elevated level, with values remaining as high as 0.45 and 0.42 S/m after 8 and 12 h of incubation, respectively. There was no significant (>5%) change in the specific membrane capacitance between these time points, with values of 9.0 (±0.3) mF/m^2. K562 cells then demonstrated an elevated

Table 1
DEP results summarising the dielectric parameters measured after different incubation periods with staurosporine

Hours of incubation with staurosporine	Measured cell radius (μm)	Cytoplasmic conductivity σ (S/m)	Membrane surface conductance K_s (pS)±20%	Specific membrane capacitance C_{spec} (mF/m^2)
0 (control)	9.0	0.28 (0.27–0.32)	9	9.7 (8.9–10.6)
4	8.0	0.450 (0.40–0.50)	12	10.0 (8.0–11.5)
8	7.6	0.450 (0.44–0.46)	16	14.9 (14.0–15.9)
12	7.6	0.420 (0.41–.43)	15	14.6 (14.1–15.0)
24	6.7			
Population 1		0.500 (0.400–0.600)	20	15.5 (13.3–17.7)
Population 2		0.030 (0.02–0.040)	20	15.5 (13.3–17.7)
Population 3		0.003 (0.002–0.004)	20	15.5 (13.3–17.7)
48	6.8			
Population 1		0.500 (0.400–0.600)	20	19.9 (17.7–21.1)
Population 2		0.04 (0.035–0.045)	20	19.9 (17.7–21.1)
Population 3		0.003 (0.002–0.004)	20	19.9 (17.7–21.1)

The figures in parentheses indicate the range of values over which the model retains a good fit.

specific membrane capacitance (C_{spec}) at 14.9 mF/m^2 after 8 h of incubation. This parameter remained at this level for the remainder of this study.

After 24 h of incubation with staurosporine, the DEP results indicated the presence of more than one population accounting for the different dielectric properties obtained. As shown in Table 1, each population exhibited a different cytoplasmic conductivity. Values started from 0.5 S/m, for population 1 (comprising approximately 16% of the population total), indicating that these cells possessed a high ionic strength. Population 2 (5% of total) demonstrated a reduced cytoplasmic conductivity of 0.03 S/m, which might indicate cells later in the apoptotic process, whilst population 3 (79% of total) showed a cytoplasmic conductivity of 0.003 S/m, indicating that the cells are very likely to be very late-stage apoptotic, or even be necrotic. After 48 h of exposure to staurosporine, the DEP results indicated that these three cell populations were again present. At this time point, the ratio of populations was as follows: population 1, 14% of total; population 2, 11% of total; population 3, 75% of total. Values of C_{spec} were elicited for all three populations as shown in Table 1.

The annexin V data for K562 at different incubation periods with staurosporine showed that approximately 87% of cells were in the viable region before staurosporine treatment. After 4 h of treatment, the cytogram showed a slight increase in the expression of PS (corresponding to a shift in cells to the right of the cytogram) relative to the control untreated cells, and a general diminution in the number of cells observed. No significant change was observed until 24 h after treatment (Fig. 4), when the presence of 3 populations of varying numbers emerged. The population analysis was suggestive of a significant number of cells being in the late apoptotic stage (19%) relative to the early apoptotic stage (5%). At the 24-h time point, approximately 52% of the population seemed to be viable. After 48 h of treatment, the cytogram (not shown) indicated that 25% of the population were in the late apoptotic/necrotic stage, compared to 21% in the early apoptotic region and 28% in the viable region.

When using TMRE, it was found that incubating the cells with staurosporine produced changes in the $\Delta\Psi_m$ after 4 h of exposure, causing the peak to shift slightly to the right (seen in Fig. 3A) in comparison with the TMRE only treated cells (Fig. 2A), indicating a slight increase in $\Delta\Psi_m$ corresponding to a hyperpolarised state. The data maintained this trend until 24 h elapsed (Fig. 4A), at which point the data indicated the presence of more than one population; one of these produced a peak shift to the right (hyperpolarisation) and the other had a peak that shifted to the left (depolarisation) relative to the control.

4. Discussion

As outlined previously, there is a high degree of similarity in the results observed between 4 and 12 h of exposure, and between 24 and 48 exposure. In order to discuss these effects separately, we here consider the observations in light of known effects of early and late apoptosis, respectively.

4.1. Early apoptosis

The DEP results highlighted an increased ionic concentration in the cytoplasm following 4 h of incubation with staurosporine relative to untreated cells. This was indicated by a sharp rise in conductivity from 0.28 S/m to 0.4 S/m, respectively (Table 1). The increased cytoplasmic conductivity persisted over the first 12 h of incubation. Furthermore, the TMRE assay demonstrated a slight mitochondrial membrane potential (MMP) hyperpolarisation. This has been reported in several previous studies [4,11,34]; a recent study [6] showed that Lactacystin-induced apoptosis in rat retinal pigment epithelial cell line (RPE)-J is closely associated with an early mitochondrial hyperpolarisation induced by intracellular alkalinisation. We suggest that the most likely mechanism may involve ionic *efflux*. Although the early events triggering apoptosis are still poorly understood [35], a number of studies have reported a dramatic decrease in

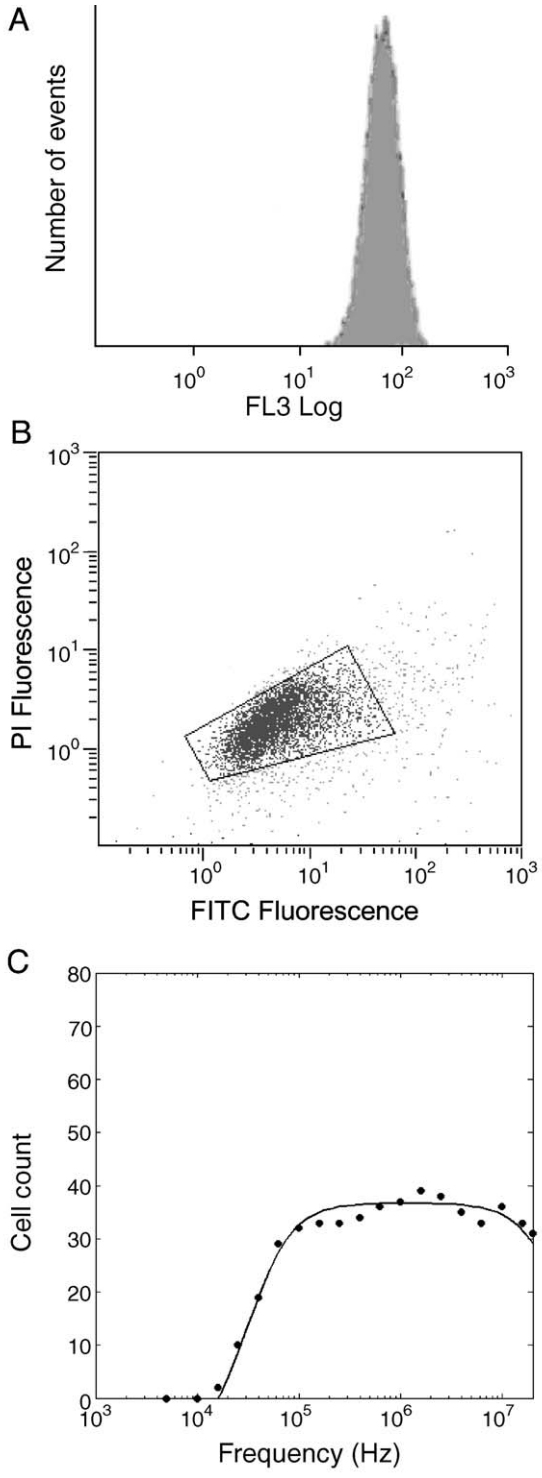

Fig. 3. The TMRE (A), Annexin-V (B) and DEP spectrum data (C) for cells after exposure to staurosporine for 4 h. There is a slight shift to the right in the TMRE data indicating membrane hyperpolarisation, whilst the DEP spectrum remains at a plateau to higher frequencies indicating increased cytoplasm conductivity.

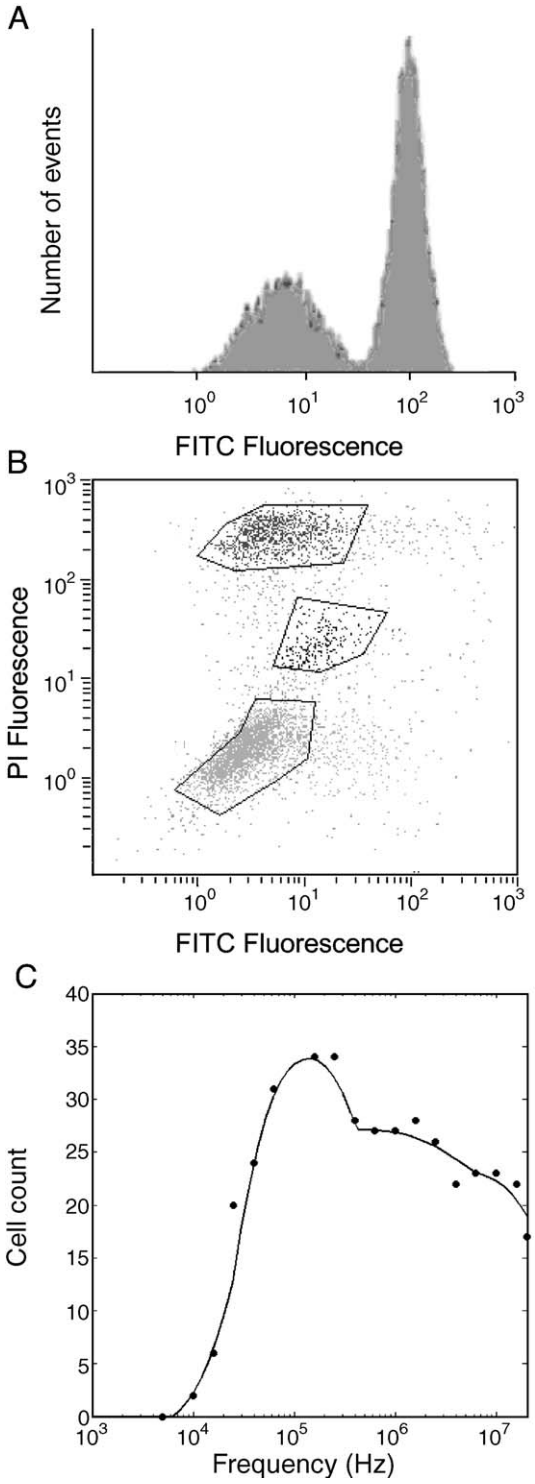

Fig. 4. The TMRE (A), Annexin-V (B) and DEP spectrum data (C) for cells exposed to staurosporine for 24 h. The hyperpolarised cells in the TMRE data are joined by a depolarised subpopulation, whilst multiple populations are visible in both the DEP and Annexin-V data. In the Annexin cytograph, the three populations appear as clusters from low to high along the centre of the image, with gated regions containing 19%, 5% and 52%, top to bottom. In the DEP spectrum, the best fit is provided by superimposing three subpopulations (shown in the side figures) corresponding to different values of cytoplasmic conductivity.

the intracellular ions during apoptosis, primarily K^+ and Na^+ [36]. The loss of K^+ was reported to be as high as 95% [37], whilst others have reported K^+ levels falling from 150 to 50 mM in a fibroblast cell line [38], and 35 mM in shrunken apoptotic thymocytes [39]. The same phenomenon is reported in other cell

lines in apoptosis, including lymphocytes [40], lymphoma cells [7] and in Jurkat cells [41].

The efflux of K^+ accompanied by the efflux of Cl^- permits the osmotic movement of water out of the cell, generating a characteristic loss of cell volume (apoptotic volume decrease, AVD) [35]. Apoptotic cell shrinkage has also been associated with a decrease in the intracellular K^+ and Na^+ [36]. This loss of cytosolic K^+ occurs before cell shrinkage, consistent with a role for K^+ efflux in cell volume reduction, and K^+ loss was also seen before the production of reactive oxygen species [12]. Maeno and colleagues [42] reported an approximate 30% loss in cell volume in HeLa and U937 cells 4 h after treatment with staurosporine.

We suggest that the possible mechanism of increase in cytoplasmic conductivity relates to the loss of cell volume. It can be noted that the increase in conductivity (which is proportional to ionic concentration, and hence inversely proportional to cytoplasmic volume) seen from the DEP data corresponds closely with the loss of the cell volume as a result of ionic efflux and water loss; it may be postulated that this causes the remaining cytosolic ions (particularly those related to intracellular macromolecules) to become more concentrated inside the cell, whilst the reduction in volume in line with the reduction in K^+ means that the conductivity component due to K^+ also remains significant.

The DEP results obtained in this study highlight significant changes in the specific membrane capacitance, which increased following staurosporine treatment from around 10.0 to 14.9 mF/m^2 (for 4 and 12 h following treatment, respectively). This is consistent with the actual surface area of the cell being maintained during cell shrinkage, causing a rise in the net capacitance per unit area when considering the shrunken cell as a perfect (rather than ruffled) sphere, and the fact that the cells are known to become significantly more folded (and less spherical) during apoptosis. The capacitance remained high up to 12 h after the start of staurosporine treatment. Generally, the surface conductance did not vary significantly during this stage of apoptosis.

Interestingly, our results contrast sharply with those of the previous study of dielectric changes of apoptotic cells by Wang et al. [27], who reported a significant decrease in the membrane capacitance during early apoptosis, with a concomitant increase in the crossover frequency (rather than the decrease seen here). One possible explanation is that the morphological differences caused by apoptosis are different in the HL-60 cells used, as Wang et al. [27] did not describe any change in cell radius during the apoptotic process, whereas K562 cells show significant cell shrinkage. This may lead to a smoothing effect (and reduction in capacitance) in the HL-60s, whilst K562 cells increase in membrane area relative to cell volume and hence increase capacitance.

One potentially important factor to consider is that the K^+ efflux may increase the ionic content of the medium, causing an anomalous result by increasing the medium conductivity. We believe that the experimental protocol of resuspending the cells into low-conductivity medium immediately before experimentation should have minimised this effect. It is known that the calculation of cytoplasmic conductivity is independent of medium conductivity [33], so that any influence in the results would be observed in the calculation of the membrane parameters. However, the increase in membrane capacitance observed is entirely in line with predictions due to cell shrinkage, indicating that variation in medium conductivity during the experiment is unlikely to have occurred.

4.2. Late apoptosis

DEP revealed that after 24 h of incubation with staurosporine, more than one cell population was present; multiple populations were also seen after 48 h of incubation with staurosporine. The dielectric parameters extracted from these populations at the two time points are summarised in Table 1. After 24 h of treatment, DEP results showed the presence of 3 populations, believed to be dead/necrotic cells where the cytoplasmic conductivity was very low; a depolarised population with low cytoplasmic conductivity consisting of possibly late apoptotic cells, and a highly-conductive population that is still behaving as if in early apoptosis. The cytoplasmic conductivities of these three populations were 0.003, 0.03 and 0.50 S/m, respectively. Similarly, three populations could also be observed in the Annexin V assay data. On the other hand, TMRE data showed the presence of two sub-populations with the appearance of a subpopulation with depolarised MMP in addition to the hyperpolarised subpopulation (Fig. 4a). Similar results were observed for 48 h, except for a shift in cell numbers towards necrotic cells. The Annexin V data showed similar results to those observed at 24 h, with a greater population in the "late apoptotic" group.

Considering the hypothesis proposed earlier for elevated cytoplasmic conductivity, we would anticipate that those cells still in early apoptosis form the basis of hyperpolarised population 1. Population 2 was strongly depolarised, suggesting cells reaching the end of the apoptotic cycle where the ionic efflux is over-riding reductions in size and corresponding ion concentration; it is notable that rather than a "smeared-out" dispersion, the results strongly indicated a population with approximately the same value of cytoplasmic conductivity, indicating that in these cells it is indicative of a distinct physiological state. The very low conductivity of population 3 is indicative of dead necrotic cells, whose plasma membranes had ruptured. This trend was observed again at 48 h, where there was an increase in proportion of cells in late apoptosis and a decrease in cells in necrosis, possibly indicating that the necrotic population was undergoing fragmentation at the end of the apoptotic process. When comparing the numbers of cells identified in different populations by DEP and flow cytometry, there are some discrepancies. The most significant difference was that the proportion of cells in the necrotic stage was reported as being much higher when assessed by DEP. We suggest that this may be due to the relatively gentle manner in which cells are manipulated by DEP; flow cytometry involves high shear forces which could potentially break up cells in the final stages of apoptosis, when the apoptotic bodies have been formed and can easily break off, reducing the cell to small

fragments whose fluorescence is below the threshold level for analysis. The second discrepancy was that DEP reported a greater proportion of cells entering late apoptosis than Annexin V; this is consistent with the flow cytometric approach being relatively insensitive to the early onset of apoptosis, with the cells gradually emerging from a general healthy/early apoptotic cluster after 24 h. After 48 h, this process was presumably complete, as the ratio of these populations was much closer.

As in the previous section, the specific membrane capacitance of the three populations after 48 h treatment remained elevated, reflecting the folded membrane morphology and size changes; the values are commensurate with the maintenance of surface area for a given change in radius, and morphological changes may include membrane folding or production of apoptotic bodies [43]. This is particularly evident in the highly elevated value (19.9 mF/m^2) in the population after 48 h.

5. Conclusions

DEP can be used as a rapid, non-invasive technique to detect early apoptotic changes in cell systems. Furthermore, it can be used to differentiate between multiple populations on the basis of their dielectric properties and, therefore, gives an accurate assessment of key stages within apoptosis. The ability to perform such an assessment on a population of cells simultaneously demonstrates the applicability of electrokinetic assays for apoptosis, particular in a high throughput setting by parallelising the measurements [44]. Our data indicate that K562 cells increase in cytoplasmic conductivity within the first 4 h of exposure to staurosporine, an effect that persists beyond 12 h. The Annexin V assay indicated that this occurred synchronously with early-stage apoptosis. Furthermore, within this time period, TMRE data pointed to hyperpolarisation in the MMP.

Although no work exists which directly explains the rise of cytoplasmic conductivity at this stage of apoptosis, a number of known events may underlie this observation. The most likely cause of this effect is cell shrinkage due to water loss triggered by ion (K^+, Cl^-) efflux, resulting in an increase in the intracellular concentration of the remaining ions. After 24 and 48 h of incubation with staurosporine, multiple populations were detected by DEP, highlighting the dielectric changes that the cell undergoes before death or necrosis. The Annexin V results showed that the majority of cells were identified as being in the late stages of apoptosis and the TMRE data indicated both depolarised and hyperpolarised MMP in the population. The DEP results at these two time points showed cells with elevated, diminished and depleted cytoplasmic conductivities after 24 h of exposure to staurosporine. The reduction effect might be associated with the later stages of apoptosis. However, this conductivity was significantly higher than the third population (assumed to be dead cells). Further and closer examination of our experimental model using pharmacological blockers to eliminate specific changes seen, and the incorporation of other apoptosis-inducing compounds, will help to further elucidate the precise mechanisms underlying these observations.

Acknowledgements

We thank Professor Ronald Pethig and Drs George Kass, Kai Hoettges and Patricia Pirard for valuable discussions, and the Engineering and Physical Sciences Research Council for a scholarship to FHL.

References

[1] C.B. Thompson, Apoptosis in the pathogenesis and treatment of disease, Science 267 (1995) 1456–1462.
[2] J.F. Kerr, A.H. Wyllie, A.R. Currie, Apoptosis: a basic biological phenomenon with wide-ranging implications in tissue kinetics, Br. J. Cancer 26 (1972) 239–257.
[3] D. Hughes, H. Mehmet, Cell Proliferation and Apoptosis. Advanced Methods, Bios Scientific Publishers Limited, Oxford, 2003.
[4] D.R. Green, J.C. Reed, Mitochondria and apoptosis, Science 281 (1998) 1309–1312.
[5] A.R. Khaled, D.A. Reynolds, H.A. Young, C.B. Thompson, K. Muegge, S. K. Durum, Interleukin-3 withdrawal induces an early increase in MMP unrelated to the bcl-2 family—Roles of intracellular pH, ADP transport, and F0F1-ATPase, J. Biol. Chem. 276 (2001) 6453–64624;
A.R. Khaled, A.N. Moor, A.Q. Li, D.K. Ferris, K. Muegge, R.J. Fisher, L. Fliegel, S.K. Durum, Trophic factor withdrawal: p38 mitogen-activated protein kinase activates NHE1, which induces intracellular alkalinization, Mol. Cell. Biol. 21 (2001) 7545–7557.
[6] J.M. Kim, H.R. Bae, B.S. Park, J.M. Lee, H.B. Ahn, J.H. Rho, K.W. Yoo, W.C. Park, S.H. Rho, H.S. Yoon, Y.H. Yoo, Early mitochondrial hyperpolarization and intracellular alkalinisation in lactacystin-induced apoptosis of retinal pigment, J. Pharmacol. Exp. Ther. 305 (2003) 474–481.
[7] C.D. Bortner, F.M. Hughes Jr., J.A. Cidlowski, A primary role for K^+ and Na^+ efflux in the activation of apoptosis, J. Biol. Chem. 272 (1997) 32436–32442.
[8] S.P. Yu, C.H. Yeh, S.L. Sensi, B.J. Gwag, L.M.T. Canzoniero, Z.S. Farhangrazi, H.S. Ying, M. Tian, L.L. Dugan, D.W. Choi, Mediation of neuronal apoptosis by enhancement of outward potassium current, Science 278 (1997) 114–117.
[9] S.P. Yu, C.H. Yeh, U. Strasser, M. Tian, D.W. Choi, NMDA receptor mediated K^+ efflux and neuronal apoptosis, Science 284 (1999) 336–339.
[10] C.D. Bortner, J.A. Cidlowski, Uncoupling cell shrinkage from apoptosis reveals that Na+ influx is required for volume loss during programmed cell death, J. Biol. Chem. 278 (2003) 39176–39184.
[11] P.F. Li, R. Dietz, R. von Harsdorf, p53 regulates mitochondrial membrane potential through reactive oxygen species and induces cytochrome c-independent apoptosis blocked by Bcl-2, Eur. Mol. Biol. Org. J. 18 (1999) 6027–6063.
[12] B. Dallaporta, T. Hirsch, S.A. Susin, N. Zamzami, N. Larochette, C. Brenner, I. Marzo, G. Kroemer, Potassium leakage during the apoptotic degradation phase, J. Immunol. 160 (1998) 5605–5615.
[13] A.H. Wyllie, J.F.R. Kerr, A.R. Currie, Cell death: the significance of apoptosis, Int. Rev. Cytol. 68 (1980) 251–306.
[14] H.A. Pohl, Dielectrophoresis, Cambridge Univ. Press, Cambridge, 2003.
[15] T.B. Jones, Electromechanics of Particles, Cambridge Univ. Press, Cambridge, 1995.
[16] M.P. Hughes, Nanoelectromechanics in Engineering and Biology, CRC Press, Boca Raton, 2002.
[17] X. Hu, W.M. Arnold, U. Zimmermann, Alterations in the electrical-properties of lymphocyte-T and lymphocyte-B membranes induced by mitogenic stimulation-activation monitored by electro-rotation of single cells, Biochim. Biophys. Acta 1021 (1990) 191–200.
[18] J.P.H. Burt, R. Pethig, P.R.C. Gascoyne, F.F. Becker, Dielectrophoretic characterization of friend murine erythroleukaemic cells as a measure of induced-differentiation, Biochim. Biophys. Acta 1034 (1999) 93–101.
[19] P.R.C. Gascoyne, Y. Huang, R. Pethig, J. Vykoukal, F.F. Becker,

Dielectrophoretic separation of mammalian-cells studied by computerized image-analysis, Meas. Sci. Technol. 3 (1992) 439–445.
[20] P.R.C. Gascoyne, R. Pethig, J. Burt, F.F. Becker, Membrane-changes accompanying the induced-differentiation of friend murine erythroleukemia-cells studied by dielectrophoresis, Biochim. Biophys. Acta 1149 (1993) 119–126.
[21] F.F. Becker, X.-B. Wang, Y. Huang, R. Pethig, J. Vykoukal, P.R.C. Gascoyne, The removal of human leukaemia-cells from blood using interdigitated microelectrodes, J. Phys., D, Appl. Phys. 27 (1994) 2659–2662.
[22] P.R.C. Gascoyne, X.-B. Wang, Y. Huang, F. Becker, Dielectrophoretic separation of cancer cells from blood, IEEE Trans. Ind. Appl. 33 (1997) 670–678.
[23] X.-B. Wang, Y. Huang, X.J. Wang, F. Becker, P.R.C. Gascoyne, Dielectrophoretic manipulation of cells with spiral electrodes, Biophys. J. 72 (1997) 1887–1899.
[24] X.-B. Wang, J. Yang, P.R.C. Gascoyne, Role of peroxidase in AC electrical field exposure effects on Friend murine erythroleukemia cells during dielectrophoretic manipulations, Biochim. Biophys. Acta 1426 (1999) 53–58.
[25] M. Cristofanilli, G. De Gasperis, L.S. Zhang, M.C. Hung, P.R.C. Gascoyne, G.N. Hortobagyi, Automated electrorotation to reveal dielectric variations related to HER-2/neu overexpression in MCF-7 sublines, Clin. Cancer Res. 8 (2002) 615–619.
[26] F.H. Labeed, H.M. Coley, H. Thomas, M.P. Hughes, Assessment of multidrug resistance reversal using dielectrophoresis and flow cytometry, Biophys. J. 85 (2003) 2028–2034.
[27] X.J. Wang, F.F. Becker, P.R.C. Gascoyne, Membrane dielectric changes indicate induced apoptosis in HL-60 cells more sensitively than surface phosphatidylserine expression or DNA fragmentation, Biochim. Biophys. Acta 1564 (2002) 412–420.
[28] V.A. Fadok, D.R. Voelker, P.A. Campbell, J.J. Cohen, D.L. Bratton, P.M. Henson, Exposure of phosphatidylserine on the surface of apoptotic lymphocytes triggers specific recognition and removal by macrophages, J. Immunol. 148 (1992) 2207–2216.
[29] S.J. Martin, C.P.M. Reutelingsperger, A.J. Mcgahon, J.A. Rader, R.C.A.A. Vanschie, D.M. Laface, D.R. Green, Early redistribution of plasma membrane phosphatidylserine is a general feature of apoptosis regardless of the initiating stimulus inhibition by overexpression of bcl-2 and ABL, J. Exp. Med. 182 (1995) 1545–1556.
[30] B. Ehrenberg, V. Montana, M.D. Wei, J.P. Wuskell, L.M. Loew, Membrane potential can be determined in individual cells from the nernstian distribution of cationic dyes, Biophys. J. 53 (1988) 785–794.
[31] J. Martin, K. Mahlke, N. Pfanner, Role of an energised inner membrane mitochondrial protein import, J. Biol. Chem. 266 (1991) 18051–18057.
[32] F. Gartner, W. Voos, A. Querol, B.R. Miller, E.A. Craig, M.G. Cumksy, N. Pfanner, Mitochondrial import of subunit Va of cytochrome c oxidase characterised with yeast mutants, J. Biol. Chem. 270 (1995) 3788–3795.
[33] L.M. Broche, F.H. Labeed, M.P. Hughes, Extraction of dielectric properties of multiple populations from dielectrophoretic collection spectrum data, Phys. Med. Biol. 50 (2005) 2267–2274.
[34] I. Marzo, C. Brenner, N. Zamzami, J.M. Jurgensmeier, S.A. Susin, H.L.A. Vieira, M.C. Prevost, Z.H. Xie, S. Matsuyama, J.C. Reed, G. Kroemer, Bax and adenine nucleotide translocator cooperate in the mitochondrial control of apoptosis, Science 281 (1998) 2027–2031.
[35] A.M. Porcelli, A. Ghelli, C. Zanna, P. Valente, S. Ferroni, M. Rugolo, Staurosporine induces apoptotic volume decrease (AVD) in ECV304 cells, Ann. N. Y. Acad. Sci. 1010 (2003) 342–346.
[36] J.V. McCarthy, T.G. Cotter, Cell shrinkage and apoptosis: a role for potassium and sodium ion efflux, Cell Death Differ. 4 (1997) 756–770.
[37] F.M. Hughes Jr., C.D. Bortner, G.D. Purdy, J.A. Cidlowski, Intracellular K+ suppresses the activation of apoptosis in lymphocytes, J. Biol. Chem. 272 (1997) 30567–30576.
[38] G. Barbiero, F. Duranti, G. Bonelli, J.S. Amenta, F.M. Baccino, Intracellular ionic variations in the apoptotic death of L cells by inhibitors of cell cycle progression, Exp. Cell Res. 217 (1995) 410–418.
[39] F.M. Hughes Jr., J.A. Cidlowski, Potassium is a critical regulator of apoptotic enzymes in vitro and in vivo, Adv. Enzyme Regul. 39 (1999) 157–171.
[40] J.W. Montague, C.D. Bortner, F.M. Hughes, J.A. Cidlowski, A necessary role for reduced intracellular potassium during the DNA degradation phase of apoptosis, Steroids 64 (1999) 563–569.
[41] M. Gomez-Angelats, C.D. Bortner, J.A. Cidlowski, Protein kinase C (PKC) inhibits fas receptor-induced apoptosis through modulation of the loss of K+ and cell shrinkage, J. Biol. Chem. 275 (2000) 19609–19619.
[42] E. Maeno, Y. Ishizaki, T. Kanaseki, A. Hazama, Y. Okada, Normotonic cell shrinkage because of disordered volume regulation is an early prerequisite to apoptosis, Proc. Nat. Acad. Sci. U. S. A. 97 (2000) 9487–9492.
[43] B.F. Trump, I.K. Berezesky, The role of altered [Ca2+]I regulation in apoptosis, oncosis and necrosis, Biochim. Biophys. Acta 1313 (1996) 173–178.
[44] Y. Hübner, K.F. Berezes, G.E.N. Kass, S.L. Ogin, M.P. Hughes, Parallel measurements of drug actions on Erythrocytes by dielectrophoresis, using a novel 3-dimensional electrode design, IEE Proc. Nanobiotechnol. 4 (2005) 21–25.